Journal of Nanoparticle Research (2005) 7: 409–433
DOI 10.1007/s11051-005-6931-x

Nanoparticulate iron oxide minerals in soils and sediments: unique properties and contaminant scavenging mechanisms

Glenn A. Waychunas[1], Christopher S. Kim[1,2,3] and Jillian F. Banfield[1,2]
[1]*Earth Sciences Division, Lawrence Berkeley National Laboratory, Berkeley, CA 94720, USA (Tel.: +1-510-495-2224; E-mail: GAWaychunas@lbl.gov);* [2]*Department of Earth and Planetary Sciences, University of California at Berkeley, Berkeley, CA 94720, USA;* [3]*Department of Physical Sciences, Chapman University, Orange, CA 92866, USA*

Received 27 April 2005; accepted in revised form 3 May 2005

Key words: aggregation/growth, contaminant, ferrihydrite, goethite, hematite, oxide, schwertmannite, sorption colloids, water quality

Abstract

Nanoparticulate goethite, akaganeite, hematite, ferrihydrite and schwertmannite are important constituents of soils, sediments and mine drainage outflows. These minerals have high sorption capacities for metal and anionic contaminants such as arsenic, chromium, lead, mercury and selenium. Contaminant sequestration is accomplished mainly by surface complexation, but aggregation of particles may encapsulate sorbed surface species into the multigrain interior interfaces, with significant consequences for contaminant dispersal or remediation processes. Particularly for particle sizes on the order of 1–10 nm, the sorption capacity and surface molecular structure also may differ in important ways from bulk material. We review the factors affecting geochemical reactivity of these nanophases, focusing on the ways they may remove toxins from the environment, and include recent results of studies on nanogoethite growth, aggregation and sorption processes.

Introduction

Fe oxides (hematite, magnetite), oxyhydroxides (goethite, akaganeite, lepidocrocite, feroxyhyte) and hydrous oxides (ferrihydrite, hydrohematite, maghemite) [in this paper together abbreviated "FeOX"] have important roles in biogeochemical processes at the Earth's surface. This is due to their wide occurrence, tendency to nucleate and grow on the surfaces of other phases, important redox capabilities, and relatively high reactivity. As the most abundant crustal transition metal (representing 6% of the chemical composition of the Earth's crust), Fe is commonly leached from minerals by both inorganic weathering processes and biological activity (Barker et al., 1998), resulting in thre concentrated FeOX phases found in nearly all surficial soils and sediments (White & Brantley, 1995). One of the main reactions for producing FeOX phases in the environment is the oxidation of dissolved iron. Leached Fe(II) in reducing, anaerobic conditions has a relatively high solubility in pH 7 waters, with the saturation concentration of the Fe(II) hexaaquo species approaching 0.5 M at room temperature. However, dissolved Fe concentrations drop below 10^{-12} M if the Fe(II) is oxidized to the hexaaquo Fe(III) or polymerized species (Baes & Mesmer, 1976). This reaction, which occurs when ground water reaches the surface (or due to mixing of subsurface fluids) and

abundant dissolved O_2, results in the precipitation of FeOX and is commonly observed at natural springs [$Fe(II)(aq) + 1/4\ O_2 + 5/2\,H_2O \rightarrow Fe(III)(OH)_3 + 2H^+$]. Iron oxyhydroxides can also form under anaerobic conditions, for example, when iron oxidation is coupled to nitrate reduction (Straub et al., 1996). This reaction, and iron oxidation in microaerophilic environments, is often catalyzed by microorganisms. Consequently, the mineral products are frequently associated in the environment with cell surfaces and extracellular polymers (e.g., Chan et al., 2004).

Another process generating FeOX is the oxidation of pyrite (FeS_2). In pyrite-rich rocks such as those associated with ore deposits, this can lead to environmental contamination known as acid mine drainage. Oxidation of sulfide generates solutions that are quite acidic (pH $\sim$2 or less) and that carry high concentrations of both dissolved Fe(II) and Fe(III). The reaction [$FeS_2 + 7/2\,O_2 + H_2O \rightarrow Fe(II)(aq) + 2SO_4^{2-} + 2H^+$] generates aqueous Fe(II), and Fe(III) is formed by reaction with dissolved oxygen. However, low solubility of O_2 in these liquids and the slow rate of inorganic oxidation from ferrous ion to ferric ion by oxygen allow Fe(II) concentrations on the order of 0.5 M. The Fe(II) can be oxidized by mixing of mine waters with surface oxygenated water, or catalyzed by microbial activity (Edwards et al., 2000) to produce large quantities of nanoparticulate FeOX.

Fe(III) phases which form from solution begin as small clusters of octahedral Fe (O, OH, OH_2)$_6$ units that evolve into larger polymeric units with time, eventually reaching colloidal sizes (Combes et al., 1989). The driving force for aggregation and/or crystal growth of these particles is the decrease in surface energy. However, for ferrihydrite, goethite and possibly other Fe phases, the surface energy appears to be low enough (Navrotsky, 2001) that nano- to micro-size particles are metastable with respect to further growth, and crystallites larger than a few microns are exceptional. Similarly, aggregates of small particles may be metastable with respect to larger crystallites or other Fe phases and persist for long periods. It is thus possible to have significant concentrations of nanophase FeOX in sediments due to rapid formation with slow growth or transformation kinetics. A process that may affect Fe(III) phase development is the cycling created by the coupled action of iron-reducing bacteria and reoxidation.

Microorganisms can couple the reduction of ferrihydrite, goethite and other FeOX phases to the oxidation of organic carbon. The resultant Fe(II) can be sequestered in FeS phases or is free to be transported and eventually oxidized. Thus, FeOX colloids can reform, sink, form sediments, and the process is repeated. All such nanoparticulate phases are expected to possess properties markedly different from larger crystallites for the following reasons:

(1) They have large surface area/volume ratios and hence present reactive surface areas disproportionately large for their volume fraction. For example, ferrihydrite is commonly found to have surface areas on the order of 50–200 m^2/g. If a sediment were to consist of such ferrihydrite and spherical sand grains of 1 mm in diameter, then the available reactive surface area of the ferrihydrite would equal that of the sand's at a concentration of only about 0.002% by volume (assuming ideal dispersal).

(2) The structure of their surfaces may differ from those of larger crystallites, leading to altered reactivity or varied crystal chemistry. This is a complex issue encompassing many factors. For example, oxide nanocrystals may possess contracted or expanded surface layers compared to bulk phases (Cheng et al., 1993; Tsunekawa et al., 2000a, 2000b), they may have surface stoichiometry different from larger crystallites, the surfaces may be corrugated or otherwise reorganized to reduce the effects of enhanced "curvature" (perhaps creating new types of surface "sites" or a higher proportion of edge/corner/step site locations), and there can be enhanced structural disorder at the surface (Zhang et al., 2003; Gilbert et al., 2004). The redox potential of surface Fe on nanoparticles may be size-dependent, or there may be a change in proton-affinity of a coordinating oxygen atom (Boily et al., 2001). This can be due to the shifting of molecular orbital/band gap energy levels due to strain effects (well known in strained-layer-superlattices, Osbourn, 1983), to quantum confinement effects (Brus, 1983), or to stoichiometric changes. Recently quantum confinement effects have been observed in α-Fe_2O_3 nanorods, with a band gap change from 2.1 eV in the bulk to 2.5 eV in the nanorods (Guo et al., 2003).

The net effect of these factors is that nanocrystallites may have dramatically different properties compared to larger crystallites, and this will be especially true when considering reactions at nanoparticle surfaces such as sorption, surface precipitation, redox reactions, and catalysis. We expect that most of these properties will modify the binding of contaminants with FeOX nanophases, and thus lead to major effects on contaminant or nutrient transport and dispersal in the environment.

These considerations lead to a set of obvious questions: What are the volumes of naturally occurring FeOX nanoparticles in specific environments, and what specific phases are present? What are the nanoparticle size ranges in natural systems? How do nanoparticle FeOX properties and structure change as a function of size? What are the lifetimes for FeOX nanoparticles prior to aggregation or growth/transformation into larger particles? What types of processes occur during aggregation, and how does this affect growth and reactive properties?

If we could answer all of these questions we would be able to confidently predict the effect of FeOX nanoparticles on geochemical systems. However, to date, there has been little study of such environmental nanoparticles, and few model studies to characterize nanophases in the laboratory. In this paper, we present new results on synthetic goethite nanoparticles from $\sim$3 to $\sim$75 nm in average size, briefly review results on other model FeOX nanoparticle studies, and speculate on the impact of Fe nanophases on aqueous water geochemistry and water quality. Consideration of the full gamut of nanoparticle property changes with size is beyond the scope of this work, but we can consider many of the important factors within the confines of one very important environmental process: sorption.

Sorption

Sorption processes on FeOX phases are due to the formation of chemical bonds with surface atoms, a process known as chemisorption. The bonds can be covalent, ionic, or mainly involve hydrogen bonds. Though there is variation in the bonding nomenclature used in the literature, we can speak generally of inner-sphere and outer-sphere types of surface complexes that are chemisorbed. Inner-sphere complexes share some of their first coordination shells with surface oxygen or anionic species. For cations the shared atom is in the ligation sphere of the cation, while for anions it would involve the oxygens of the anion itself. Outer-sphere complexes are bound to a surface by weaker electrostatic attraction and have intervening water molecules between themselves and the surface. They are thus farther from the sorbing surface. One can readily imagine intermediate cases of binding by hydrogen bonds that are weaker than inner-sphere binding, but stronger than outer-sphere binding.

Sorption processes are generally approached from different theoretical ends, with surface complexation models and electrical double layer (EDL) theory at one end, and molecular descriptions (MD-simulated or EXAFS-measured) at the other. The EDL and complexation modeling approach can be compared with laboratory sorption experiments to understand the near equilibrium behavior of sorption as a function of solution pH, ionic strength and sorption density, but molecular details such as the types and numbers of surface sites must be assumed (Davis & Kent, 1990). Molecular approaches reveal the local nature of sorption sites, but not the larger chemical picture. Hence the approaches are highly complementary. Both molecular and EDL/complexation modeling approaches suggest ways in which sorption can be affected by nanoparticle size.

Surface "curvature" and EDL failure

For nanometer-sized particles it is no longer possible to have "flat" surfaces or crystal faces of any appreciable magnitude. The surfaces of these particles must contain atomic steps that produce an irregular outline. In this case, the electrostatic conditions that define a classical EDL model break down, and local fields vary markedly with proximity to the nanoparticle. Hence with decreasing particle size, EDL-predicted sorption models may fail. From a molecular standpoint, surface curvature may allow the approach of more surface sorbants than for a flat interface. This can lead to sorption densities higher than normally predicted, or to changes in the nature of

the surface complexation geometry. The situation is akin to the planar surface of a larger crystal possessing a high density of growth steps and irregular terminations, with much favored complexation at these defect areas. Alternatively, the increased surface disorder likely in such non-planar surfaces may result in sites less favorable for sorption due to steric or electrostatic impedances, yielding lower sorption densities than predicted. Another effect of changes in the EDL could be changes in the potential across the double layer, which will affect electron transfer across the potential and thus redox activity. Besides surface curvature and irregularity, quantum confinement effects may also affect this potential (see below). Changes in nanoparticle shape may also lead to variations in colloidal stability (Qu et al., 2004).

Different surface sites and site occupations

Recent work has shown that the surfaces of hematite and corundum in equilibrium with water are altered with respect to the ideal terminated structure (Eng et al., 2000; Trainor et al., 2004). In the case of hematite, studies utilizing surface X-ray diffraction show that the (0001) and (10–12) surfaces are depleted in the octahedral Fe ions which in the normal structure would share coordination polyhedron faces with lower Fe sites. This gives rise to a surface termination with reduced Fe concentration on the (0001) face, and ''groves'' of depleted Fe sites on the (10–12) and other ''r-plane'' type surfaces. These surface adjustments thus allow active sites for surface complexation that would not occur on the so-called bulk structure terminated surfaces (Figure 1). Other possible

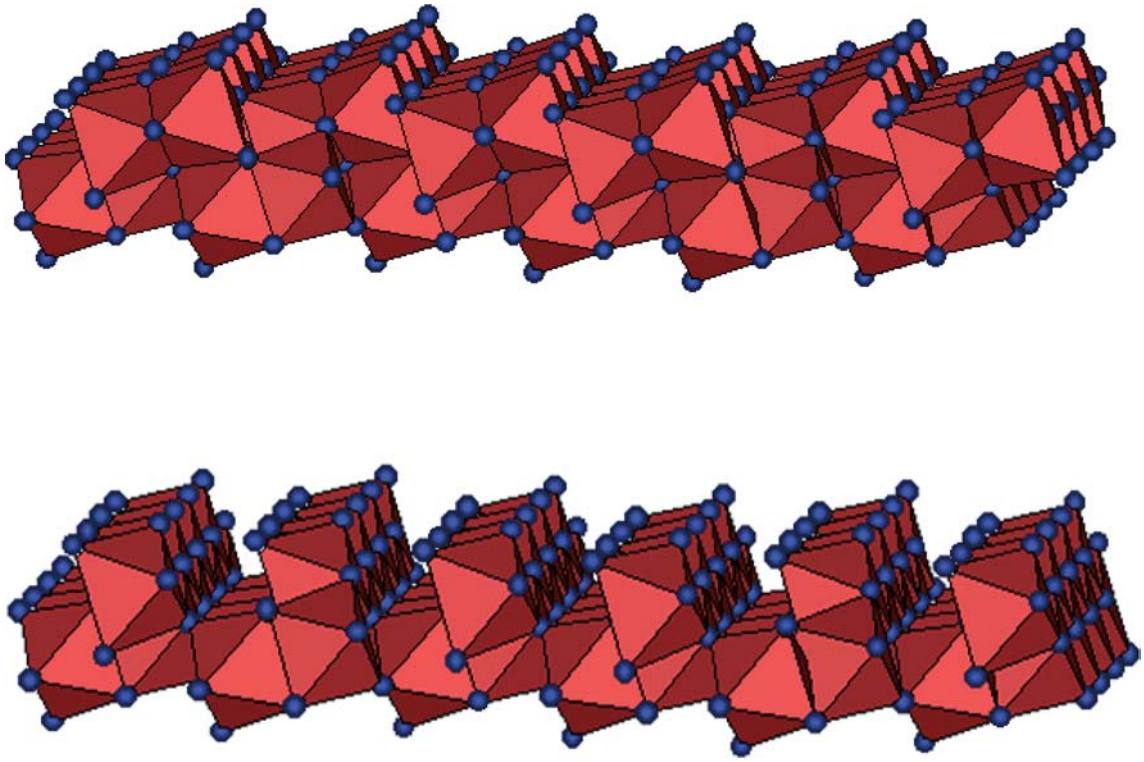

Figure 1. Top: r-plane (10-1l) type fully oxygenated ideal termination of a $3 \times 3 \times 0.5$ nm hematite particle. Bottom: same plane with Fe ions removed from the surface that share polyhedral faces with other polyhedra in the next lower layer. This type of surface change from ideal oxygen-terminated surface to reconfigured surface is observed on single hematite crystals equilibrated with neutral to acidic aqueous solutions, and indicates far more numbers and types of complexation attachment sites than would be expected in the ideal structure. In nanoparticles, additional reconfiguration, distortion and corrugation may occur to minimize surface energy or react to changes in structure.

surface changes involve reduced coordination numbers of the metal ions, which has been suggested for ferrihydrite (Zhao et al., 1994), and on nanohematite surfaces (Chen et al., 2002). In nanoparticles, other kinds of surface readjustments may be required to minimize the surface energy, e.g., reconstructions into a denser atomic structure, quasi-amorphous disordering (Gilbert et al., 2004), or complete phase transformation (see below). Thus both the types and proportions of surface sites may vary with nanoparticle size, leading to a dependence of complexation density and attachment energy on size. It is important to note that such changes may either enhance or diminish the stability of a particular surface sorption complex depending on whether the sites generated by such surface alterations are more or less hospitable to sorption.

Surface contraction or expansion

Most crystal surfaces undergo relaxation to some degree. As mineral surfaces in equilibrium with a moist atmosphere tend to be oxygen terminated, the relaxation is a response of the oxygen atoms to the absence of overlying metal cations. The loss of the cations produces an underbonding of the surface oxygens, which can be compensated in part by contraction or shortening of the lower oxygen–metal bonds (Brown & Shannon, 1973). Such contraction redistributes surface charge and affects electrostatic bonding. In nanoparticles the diameters of the particles are small enough that contraction effects can propagate through the entire particle and alter the cell dimensions (Tsunekawa et al., 2000a). This effect will alter the bulk energy of the nanoparticle and other thermodynamic properties, and can be a factor in phase transformations. Sorption is affected by surface bond length contraction via weakening of surface oxygen–complex binding, but this effect may be subtle and less important than changes in the nanoparticle phase diagram (temperature–composition–size).

Quantum confinement effects

Quantum confinement (QC) effects occur when the wave function of an excited electron or coupled electron–hole pair (exciton) carrier is near the size of the nanoparticle. Size then controls the wavefunction extent and affects band gaps and molecular orbital energies. Probably the most important effect of QC on sorption is an induced change in the rate of electron transfer from nanoparticle surface to sorption complex or aqueous solution, i.e. rate of redox reaction, as size decreases. This has been little studied in FeOX nanoparticles, but significant effects are observed in semiconductor nanoparticles (Korgel & Monbouquette, 1997; Hoffman & Hoffman, 1993) and TiO_2 nanoparticles (Toyoda & Tsuboya, 2003). Because the wavefunction of an excited electron is the size of the nanoparticle surface, all charge carriers in a semiconducting nanoparticle will be able to interact with the entire surface. This can markedly increase quantum yields for electron transfer, perhaps even to unity (Grätzel, 1989). An important consideration for FeOX nanoparticles is the possible interplay between local electronic states of the surfaces and the ''bulk'' electron states that are affected by QC. For particular types of surface topologies, QC effects may be overwhelmed by surface states (e.g., ''dangling bonds'', or local areas of unsatisfied charge, etc.). For semiconductor nanoparticles, surface complexes may affect the confinement, creating changes in physical properties. This might be exploited to ''tune'' a nanoparticle for particular reaction affinities.

Surface energy, phase stability and transformations

Critical nuclei have surface energy just offsetting bulk energy such that any increase in size will tip the energy balance in favor of the bulk energy and lead to greater thermodynamic stabilization, while a decrease in size will lead to a larger relative surface energy that will be destabilizing. The destabilizing effect can be altered if the energy components are changed by a phase (structural) transformation. For example, in TiO_2, the stable bulk phase for large crystallites is rutile, but the anatase polymorph is found to be stable at nanometer sizes. The rutile structure has the smaller bulk energy/unit volume ratio but higher relative surface energy per unit surface area. Hence at large enough surface area, a rutile nanoparticle is less stable than an anatase nanoparticle. A generalized diagram of this behavior is shown in Figure 2 (after Navrotsky, 2001), demonstrating that a size axis is required in any phase diagram involving nanometer scale materials. At extremely high surface areas, an amorphous phase may be more

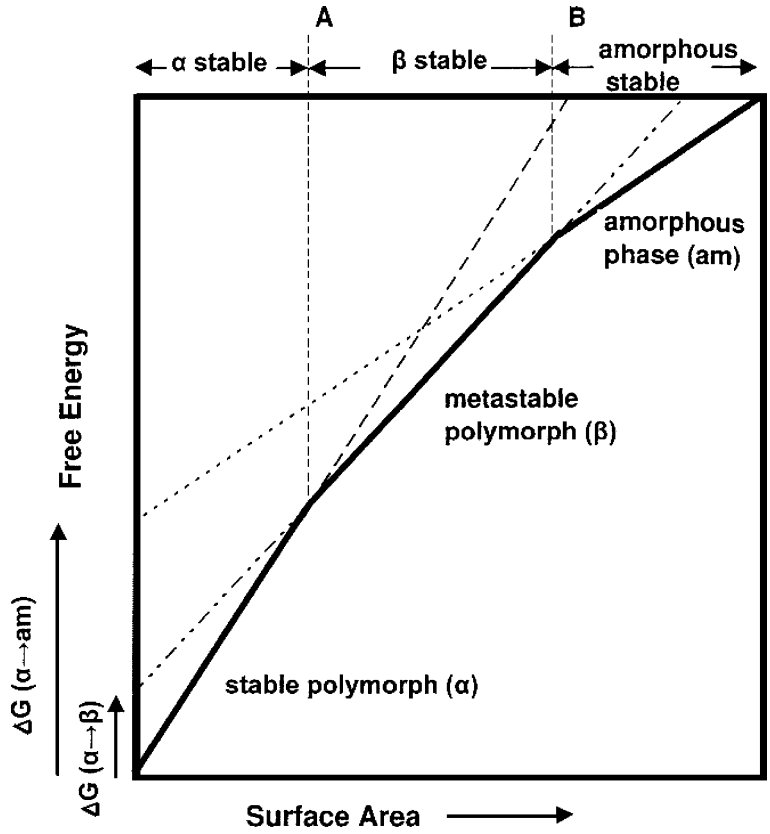

Figure 2. Model phase diagram for a nanoparticle system where surface and bulk energy contributions to the total particle free energy change considerably with respect to one another as a function of particle size. For large crystallites the stable polymorph is α. With decreasing particle size the surface energy contribution increases so that at point A the β polymorph, with lower surface energy per unit area, is favored. With further size reduction, eventually the beta phase is unstable with respect to an amorphous structure having lower surface energy per unit area (point B). All nanoparticles are metastable with respect to coarsening and adopting the alpha structure. [after Navrotsky, 2001]

stable at nanometer dimensions than any crystalline polymorph, essentially leading to a "glass transition" at low temperatures. These energy considerations dictate that a crystallite may undergo one or more structural transformations as it grows within the nanoscale regime. Phase transformations will alter the relative proportions of sorption sites and may lead to desorption of initially adsorbed species, or conversely, to enhanced uptake. A secondary effect is a likely change in P_{ZC} for the nanoparticle, which may also change sorption density at specific pH values.

Another way that surface energy can affect sorption is by a direct effect on sorbate distribution coefficients between solution and nanoparticle surfaces. If there is a sufficient energetic advantage for sorption (i.e., in cases of high nanoparticle surface energies), sorption may be driven in much the same way as growth or aggregation. This may lead to a much larger degree of contaminant sequestration on nanoparticle surfaces than would be expected from standard laboratory uptake experiments using coarser phases (Zhang et al., 1999). Such lowering of surface energy by complexation effects is possibly due on the molecular level to reductions in surface strain, distortion or other relaxation process due to the surface binding. This type of relaxation has been observed in arsenate binding to ferrihydrite (Rea et al., 1994).

Stoichiometry changes

Work on single crystal surfaces shows that the stoichiometry of hematite must change as a

function of crystallite size due to the removal of Fe(III) ions and addition of H^+ at the surfaces (Trainor et al., 2004). For example, on the (0001) surface, removal of the Fe ions whose polyhedra share faces with deeper Fe polyhedra reduces the surface layer composition to FeO_3. Protonation to balance charge would then create an $Fe(OH)_3$ surface layer. Nominally anhydrous α-Fe_2O_3 thus adds an increasing hydrous or hydroxyl component with decreasing size. For heterovalent FeOX solids like magnetite ($Fe(II)Fe(III)_2O_4$), both added hydration and a change in the ratio of metal valences may occur. One way in which valences may be changed is due to surface contraction, case (3) above. Magnetite has both Fe(III) and Fe(II) occupying octahedral FeO_6 sites. Near the surface in an anhydrous case, contraction of Fe–O distances ought to favor the shorter Fe(III)–O distances over Fe(II)–O, and hence the surface may be enriched in Fe(III). The picture is complicated by the effect of surface coordinated water which may have a stabilizing effect with an opposite bond length dependence. Electron delocalization on the vacuum surface can also affect valence states (Wiesendanger et al., 1994). For nanoparticles featuring surfaces enriched in Fe(III), the amount of Fe(II) could be dramatically decreased with a large resulting effect on physical properties such as magnetism and electrical conductivity. Changes in stoichiometry will also affect the energy needed to remove or add electrons to the conduction band, and thus change redox properties. The direct effects of such changes on sorption have not been evaluated.

Surface complexation geometry

A large number of studies have attempted to characterize the sorption of metal ions and oxyanions on FeOX using a variety of methods. EXAFS spectroscopy has been widely used because of its element selectivity – the structure near a particular sorbing complex can be directly probed regardless of the presence of other types of complexes. EXAFS spectroscopy can be applied to distinguish inner- vs. outer-sphere surface adsorption complexes, monodentate vs. bidentate linkage to the substrate, mononuclear vs. multinuclear metal surface complexes, and adsorbed vs. (co)precipitated metal species. Less direct structural information for oxyanion sorption has been obtained from IR measurements utilizing the stretching modes of the complexes. This latter method is sensitive but can suffer from interpretation problems in as much as both sorption geometry and protonation changes can lead to similar spectral changes (Myneni et al., 2004). Other types of indirect structural characterization methodologies are useful but not definitive in identifying complexation site and geometry (Sposito, 1986). A recent review of EXAFS analyses of sorption complex geometries (Brown & Sturchio, 2002) includes a very complete reference list for EXAFS studies of complexation. Table 1 comprises a subset of these results covering the complexes and geometries for the FeOX compounds that have been studied to date.

A perusal of these complexation results shows that in many cases there are multiple types of complexation geometries for the same sorbate, presumably due to differences in the exact experimental preparation conditions, variations in the crystal form of the substrate, or difficulties in spectral interpretation. A suggestive comparison is between results for ferrihydrite (hydrous ferric oxide, or HFO) and hematite or goethite. HFO, also called "2-line" ferrihydrite, is poorly crystallized having coherence sizes of about 2–5 nm in synthetic material (Janney et al., 2000). Hence we expect that comparing sorption on ferrihydrite to sorption on hematite and goethite (with crystallites more commonly in the micron size range and larger) might demonstrate the effects of reduced scale. For example, Cd(II) substitutes in the goethite structure and also forms inner-sphere complexes sharing edges with FeO_6 polyhedra (Spadini et al., 1994; Manceau et al., 2000). However in HFO, there appears only to be edge-sharing inner-sphere complexation. With Pb(II), an inner-sphere bidentate edge-sharing complex is formed on goethite (Bargar et al., 1997), but an inner-sphere multinuclear complex is formed on HFO (Manceau et al., 1992). For Se(VI) an outer-sphere complex forms on goethite (Hayes et al., 1987), but an inner-sphere bidentate complex forms on HFO (Manceau & Charlet, 1994). For arsenate $(AsO_4)^{3-}$, there are variations among types of inner-sphere complexes between the phases, including monodentate, bidentate, mononuclear and binuclear species (Waychunas et al., 1993). Finally, with Zn(II), the type of complex

Table 1. EXAFS-derived complexation geometry for selected species on FeOX substrates

Magnetite	Goethite	Hematite	Ferrihydrite/HFO	Akaganeite	Schwertmannite
Cr(VI) sorbs as Cr(III) precipitate nonepitaxial CrOOH	Cr(VI) inner-sphere monodentate and bidentate	Cr(VI) (0001) plane epitaxial precipitate or multinuclear complex	Cr(III) nonepitaxial precipitate (Cr,Fe)OOH	Cd(II) inner-sphere	Cd(II) inner-sphere
(100) plane amorphous precipitate (Cr,Fe)OOH	Cr(III) nonepitaxial precipitate (Cr,Fe)OOH	Cr(III) (0001) plane inner-sphere multinuclear	Ni(II) Ni coprecipitate		
I^- inner sphere	Cu(II) inner-sphere multidentate polymer	Pb^{2+} inner-sphere bidentate, mononuclear	Cu(II) inner-sphere bidentate		
	Zn(II) inner-sphere 4- or 6- coordinated bidentate	Lu(III) lattice substitution	Zn(II) inner-sphere bidentate 4-coordination (pH 6) outer-sphere 6-coordination		
	As(V) $(AsO_4)^{3-}$ inner-sphere bidentate, minor monodentate	As(V) $(AsO_4)^{3-}$ (0001) plane bidentate, mononuclear and binuclear (1–102) plane bidentate, mononuclear and binuclear	As(V) $(AsO_4)^{3-}$ inner-sphere bidentate		
	As(III) $(AsO_3)^{3-}$ inner-sphere bidentate	Pb(II)/malonate Ternary complex	Se(VI) $(SeO_4)^{2-}$ inner-sphere bidentate		
	Se(VI) $(SeO_4)^{2-}$ outer-sphere	U(VI) $(UO_2)^{2+}$/ Carbonate Ternary complex	Se(IV) $(SeO_3)^{2-}$ inner-sphere bidentate		
	Se(IV) $(SeO_3)^{2-}$ inner-sphere bidentate		Sr(II) outer-sphere		
	Sr(II) inner-sphere bidentate; outer-sphere		Cd(II) inner-sphere (edge sites)		
	Cd(II) lattice substitution; inner-sphere bidentate mononuclear		Pb(II) inner-sphere bidentate, multinuclear		
	Au(III) inner-sphere bidentate		Lu(III) lattice substitution		
	Hg(II) inner-sphere bidentate		U(VI) $(UO_2)^{2+}$ inner-sphere bidentate		
	Pb(II) inner-sphere bidentate mononuclear				
	Lu(III) lattice substitution				
	U(VI) $(UO_2)^{2+}$ inner-sphere bidentate				
	Np(V) $(NpO_2)^{+}$ inner-sphere				

(octahedral or tetrahedral) appears to be dependent both on substrate and pH (Trivedi et al., 2001; Waychunas et al., 2002). These differences confirm that complexation is highly substrate (and therefore surface)-dependent, and thus suggest that large changes in the type of complexation could occur in nanoparticulate phases.

Other differences between nanoparticles and bulk phases

Other important factors in understanding the extent of nanoparticle uptake and retention of species include reaction kinetics, sorption reversibility, and sequestration of sorbates. Reaction rates for sorption as a function of substrate dimension in natural systems have not been studied to our knowledge. The basic energetic factors considered earlier will affect kinetics as the relative numbers of attachment sites and the energy of binding affects the probability that a given solution complex will be sorbed and remain attached to the surface. Kinetics are also affected by competition among sorption sites, diffusion rates on the surface and through the nearby aqueous solution, and by counterion (charge balancing species) transport. Hydrological behavior within pores among nanoparticles is expected to be quite different than in larger scale systems, and flow rates may be extremely low. This is due in part to nanoscale structure in the solution near the particle, affecting the effective viscosity and rates of ligand exchanges. Hence the reactivity of the relatively large surface areas within a set of nanoparticles will be crucially affected by the degree of aggregation and the type of pore system that develops.

Reversibility of sorption reactions is strongly dependent on the degree of surface precipitation. Even a few interacting sorbed complexes will require larger proportional energies for desorption due to breaking of intercomplex bonds and entropy changes. Added to this is the tendency for surface "templating" or catalytic effects where the critical size for a precipitate nucleus is reduced on the surface. If these effects are heightened on nanoparticle surfaces there may frequently be a large hysteresis in sorption/desorption cycles, favoring development and long-term stability of additional precipitates.

Also related to sorption reversibility is the issue of "internal" sequestration or encapsulation. If oriented aggregation of nanoparticles occurs after sorption, then sorbed species may be trapped within the bonded crystallites (Banfield et al., 2000). These species cannot be desorbed in the normal sense, but will be released only if enough of the particle is dissolved that the sorbate is brought once again to the solid/water interface. It is not uncommon to find mineral crystals with extremely thin layers of impurities, nano-scale zones, or element clustering that can be detected with TEM techniques e.g., in arsenic-containing pyrite (Savage et al., 2000). Such layers or clusters preserve the host structure, but have local composition exceeding the bulk solubility for the impurity. How do these impurity regions, often just a few atomic layers in size, form initially? One possibility is that such impurities were once sorbed species forced into structural incorporation by either oriented aggregation or by an unusual burst of growth. Nanoparticles are profound subjects for such encapsulation effects, as their maximum sorption behavior may coincide with their maximum tendency for aggregation, i.e., near their surface point of zero charge (P_{ZC}), where electrostatic repulsion of particles is minimized.

Beyond possibly fostering sorption, surface precipitation and encapsulation effects, nanoparticles themselves may be vehicles for transport of pollutant and nutrients (e.g., sorbed phosphate on FeOX). This is because, unlike larger bulk particles which eventually settle out of the aqueous phase, they may readily be carried within hydrologic systems for indefinitely long distances. Hence understanding pollutant dispersal by nanophases involves not only an understanding of their unusual chemistry, surface structure and reactivity, but also the factors driving or hindering aggregation (or attachment to other larger substrates). This aspect of nanomineral behavior requires an integration of knowledge that we currently do not possess. However more and more is being learned about specific nanoparticle growth.

Nanoparticle growth

An expanding body of evidence indicates that nanoscale phases may grow through the oriented attachment [OA] of individual nanoparticles (Penn et al., 1998; Banfield et al., 2000; Gilbert et al., 2003; Guyodo et al., 2003; Huang et al., 2003;

Penn, 2004; Tsai et al., 2004; Zhang & Banfield, 2004). Oriented attachment is a specialized form of aggregation that differs dramatically from classical models of ripening-based growth from solution commonly associated with the growth of macroscale particles. Just as sorption may be influenced by surface, structural, and quantum confinement changes at nanoparticle surfaces, so may these factors play a role in the tendency for growth via OA. Most likely, some continuum between the two growth processes occurs in natural systems (Penn et al., 2001), with size serving as the determining factor for which process dominates. Aggregation-based growth at the nanoscale gives way to ripening-based growth at larger sizes, with the tipping point dependent on the particular phase, solution chemistry, and particle concentration of the system being considered.

The exact effects of aggregation-based nanoparticle growth on the retention of sorbed species, whether toxic metal cations, inorganic anion ligands, or organic contaminants, are largely unknown but may include the following:

- Migration to other mineral/water interfaces on the aggregate, thus persisting as surface sorbed species
- Encapsulation into the aggregating matrix as trapped species
- Diffusion into a nanoparticle's original pore structure or new pore spaces created by aggregation
- Incorporation into the newly-formed aggregates as structural impurities
- Formation of localized nano- or micro-precipitates within the aggregating particles
- Desorption and re-release of the sorbed species back into solution

Depending on the type of sorbed species as well as the nanoparticulate sorbent phase, different responses to nanoparticle aggregation are likely to occur in varying proportions. Therefore, understanding the behavior of sorbed species under the conditions of substrate growth has significant implications for their long-term stability. This is of particular interest when considering the remediation of contaminants, particularly those present as dissolved species in surface or groundwaters, through sorption- or (co)precipitation-based treatment strategies which effectively remove the pollutants from the aqueous phase and sequester them into the solid phase. The reductions in mobility, toxicity, and bioavailability associated with sorption combined with the enhanced levels of uptake expected of nanophases provide considerable incentive to further explore the role that nanoparticulate minerals play in the attenuation of contaminant species in the environment.

The following section provides brief summaries of our recent studies on the aggregation-based growth of goethite at the nanoscale and the effects of particle size and growth on the sorption and precipitation of toxic heavy metals. Nanoparticles of goethite have been identified as the dominant reactive oxyhydroxide phase in lake and marine sediments (van der Zee et al., 2003). Heavy metal contamination is a pervasive environmental problem in numerous areas including abandoned and inactive mines, industrial sites with legacies of unregulated dumping, geological areas naturally enriched in metals that have been disturbed by human development, and bay/delta regions suffering from the accumulation of decades of polluted runoff and sediments. Therefore, a detailed understanding of the mechanisms by which heavy metals interact with goethite nanoparticles and the extent and permanence of these interactions is essential in assessing the prospects of nanoparticle use in environmental cleanup strategies.

The brief summaries of various projects on nanoscale goethite that follow represent work that either has been recently completed or is still ongoing. As such, these sections focus on our latest results, forgoing detailed explanation of experimental methods or analytical techniques used (to be published elsewhere), in favor of presenting initial conclusions we have drawn from the data.

Macroscopic/spectroscopic characterization of nanogoethite growth

Nanoscale iron oxyhydroxides have been observed to grow through oriented attachment of individual nanoparticles in both natural (Banfield et al., 2000; Chan et al., 2004) and synthetic (Penn et al., 2001; Guyodo et al., 2003) settings. Determining the precise mechanism(s) of growth in this size regime has important implications for both our evolving understanding of aggregation-based growth as well as the practical applications of this growth process towards issues such as

contaminant sequestration. In order to minimize the complexities inherent in the natural environment, it is useful to develop a model system that allows us to study the effects of individual variables (in this case, aging time) on particle size, morphology, growth rate, and structure.

In our current work, the formation of goethite nanoparticles was induced from iron-rich solutions using a microwave-based synthesis method (Guyodo et al., 2003). The nanoparticle suspension was dialyzed to remove excess dissolved iron and then aged in an oven at 90°C for durations ranging up to 33 days. Although this method of aging and growth is clearly accelerated relative to natural growth rates in order to facilitate the generation of a wide range of differently-sized particles in a realistic time frame, comparisons of the particle aggregates with those of natural FeOX samples appear similar enough to presume that the methods of growth were not fundamentally altered through this heating process. Removing aliquots of the aging suspension at various times allows us to collect nanogoethite samples representing different aging times. These samples were then characterized by an array of analytical techniques to identify trends in specific characteristics as a function of aging/growth, namely:

- High-resolution transmission electron microscopy (TEM) (morphology, size)
- Dynamic light scattering (DLS) (average particle size)
- BET surface area analysis (reactive surface area)
- X-ray diffraction (XRD) (phase identification)
- Fe K-edge extended X-ray absorption fine structure (EXAFS) spectroscopy (average local atomic structure)

TEM analysis of samples of varying aging times reveals that the initial nanoparticles are 3–5 nm in size and oblong in shape (Figure 3a); with additional aging, direct evidence for oriented aggregation of individual nanoparticles can be observed, with the aggregates assuming a more rod-like morphology (Figure 3b). In the most aged sample studied (33 days), an abundance of these rod-shaped particles dominates, with dimensions of roughly 10×100 nm (Figure 3c); however, several of the initial nanoparticles and smaller aggregates remain as well.

A combination plot showing changes in surface area and average hydrodynamic diameter as a function of aging time (Figure 4) shows an expected inverse relationship between the two, with surface area decreasing as the average particle size increases over time. Additionally, it appears that there are two distinct stages of growth in the system, with a rapid increase in particle size between 0 and 4 days followed by slower growth from 4 to 32 days; this implies a shift in the growth mechanism between the two stages, perhaps from oriented aggregation to ripening as discussed earlier.

X-ray diffraction patterns collected from the aged samples using high-flux synchrotron-based X-rays (Figure 5) suggest that the nanoparticles do not undergo a phase change with aging, which would be observed by changes in peak positions; instead, the samples can be consistently identified as goethite throughout the aging process, with changes in peak intensity/width attributed to changes in particle size (progressively larger particles resulting in sharper and more well-defined peaks). Some of this peak shape change is the result only of particle size change and can be quantified by the Scherrer relation (Warren, 1968). However, there also appears to be an effect of decreasing degree of disorder as particle size increases, due most likely to the smaller proportion of surface-associated atoms. EXAFS results support the notion of a progressive and continuous increase in the structural ordering of the nanoparticles with aging (Figure 6). This is most clearly evidenced in the Fourier transforms of the spectra, which show an increasing intensity of the second-neighbor peaks consistent with an increased Fe–Fe coordination number and/or degree of structural ordering around the average Fe atom in the sample. The trend observed in the Fourier transforms could be interpreted as either a result of the increasing proportion of Fe atoms associated with the bulk and the declining proportion of surface-terminated Fe atoms with aging, or an actual phase transition from poorly-ordered ferrihydrite to goethite. The XRD data, however, seem to support the former explanation, with the structural classification of the nanoparticles as goethite upon initial formation and throughout the aging process.

To summarize, the application of multiple complementary techniques to characterize nanoparticulate goethite during the aging process (engendered by heating the suspension at 90°C)

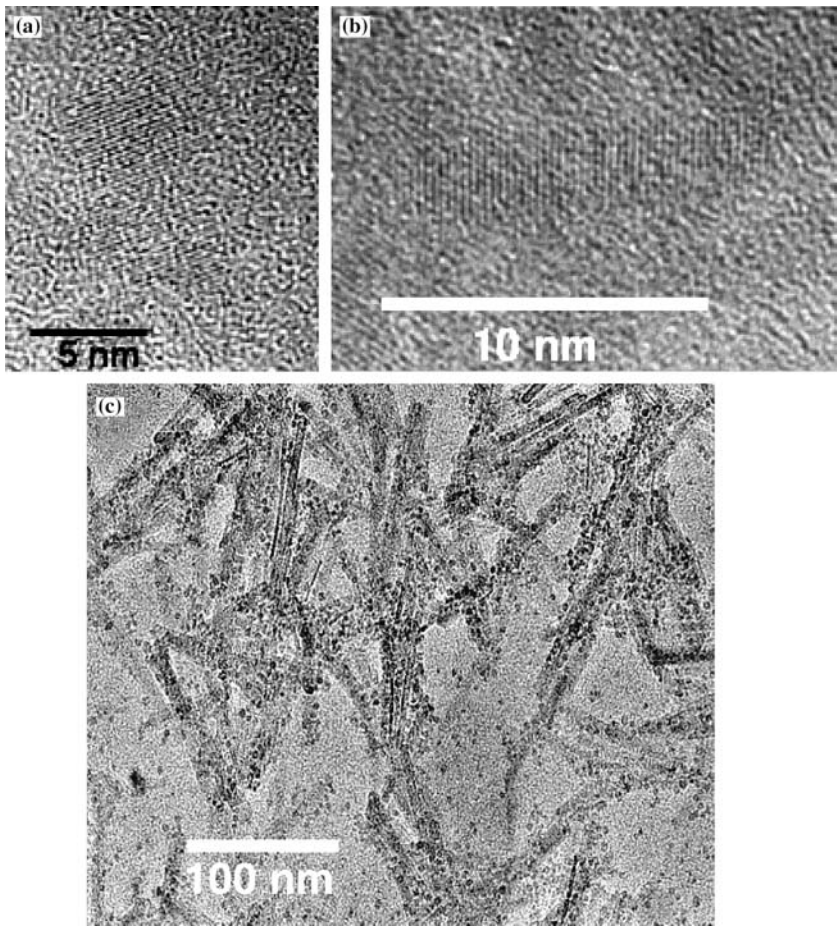

Figure 3. High-resolution (500,000×) transmission electron microscopy (TEM) images of synthetic goethite nanoparticles that have aggregated from more oblong shapes (a, showing two such particles connected through oriented attachment as viewed by their lattice fringes) to more rod-like shapes (b, where 3–4 nanoparticles have aggregated to create a different, more elongated morphology compared to the initial particles). After 33 days of aging, many such rods have formed (c) although many of the initial oblong nanoparticles remain.

yields a series of observable trends that distinguish the mechanisms of growth in the initial stages following nanoparticle formation:

- Continuous increase in particle size
- Two distinct stages of growth: a rapid growth stage within the first 4 days corresponding primarily to nanoparticle aggregation followed by a slower growth stage more likely to reflect traditional ripening-based growth mechanisms
- Change in particle morphology from oblong to rod-shaped, initially driven by the oriented aggregation of oblong particles
- Increased degree of structural ordering

Clear understanding of these trends in goethite nanoparticle growth can help us interpret similar processes in natural systems, and provide a basis for the interpretation of studies involving observations of nanoparticle growth and the influence of particle size and aging on the sorption of heavy metals in solution.

SAXS/WAXS studies of aggregation-based growth of goethite nanoparticles

The previous characterization techniques all required the *ex situ* analysis of aged nanogoethite

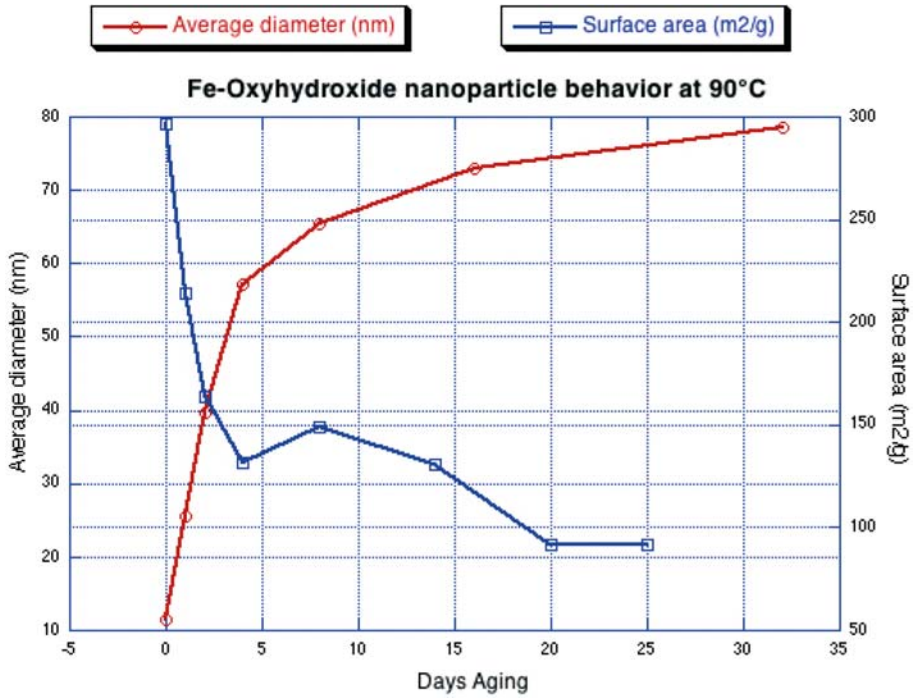

Figure 4. Combined results from initial dynamic light scattering (DLS) and BET surface area measurements of aged goethite nanoparticles, showing an inverse relationship between particle diameter and surface area.

samples which were typically dried prior to analysis, introducing the possibility of induced particle aggregation. Synchrotron-based small- and wide-angle X-ray scattering (SAXS/WAXS) provides a method of characterization that allows real-time, *in situ* observation of changes in nanoparticle size, size range, and particle structure in solution during the aging process.

For this work, goethite nanoparticles were synthesized using the microwave method cited earlier and analyzed at the 5-ID-D Dow-Northwestern-Dupont (DND) beamline at the Advanced Photon Source, Argonne National Laboratory using a simultaneous SAXS/WAXS configuration equipped with a heating stage. A suspension of the initial 3–5 nm particles was placed in a glass capillary and the temperature increased to 70°C for continuous aging; the 90°C temperature used in the previous aging experiments could not be achieved due to capillary strength and evaporation effects. SAXS/WAXS patterns were collected on the aging suspension every 15 min for a period of 12 h. To cover a wider range of aging times, SAXS/WAXS patterns were also collected on the same *ex situ* samples analyzed in earlier characterization studies; These samples were analyzed in their original suspensions, minimizing any additional aggregation that would have been induced by drying.

The processed *in situ* SAXS data show that at the outset of the aging process, most nanoparticles fall within a size range of 2–6 nm diameter (Figure 7a), corroborating the TEM images of the initial nanoparticles. With progressive aging, this dominant population of nanoparticles begins to shrink (Figure 7b) while a population of slightly larger particles featuring a broader size distribution (> 5 nm) starts to increase (Figure 7c). SAXS data from the *ex situ* samples show the continuation of this trend (Figure 8), with the initial population of nanoparticles continuing to decline over time in favor of a much broader distribution of particle sizes ranging from roughly 8–50 nm. These results provide evidence for aggregation-based growth of the initial nanoparticles, demonstrated by the direct decline in the initial

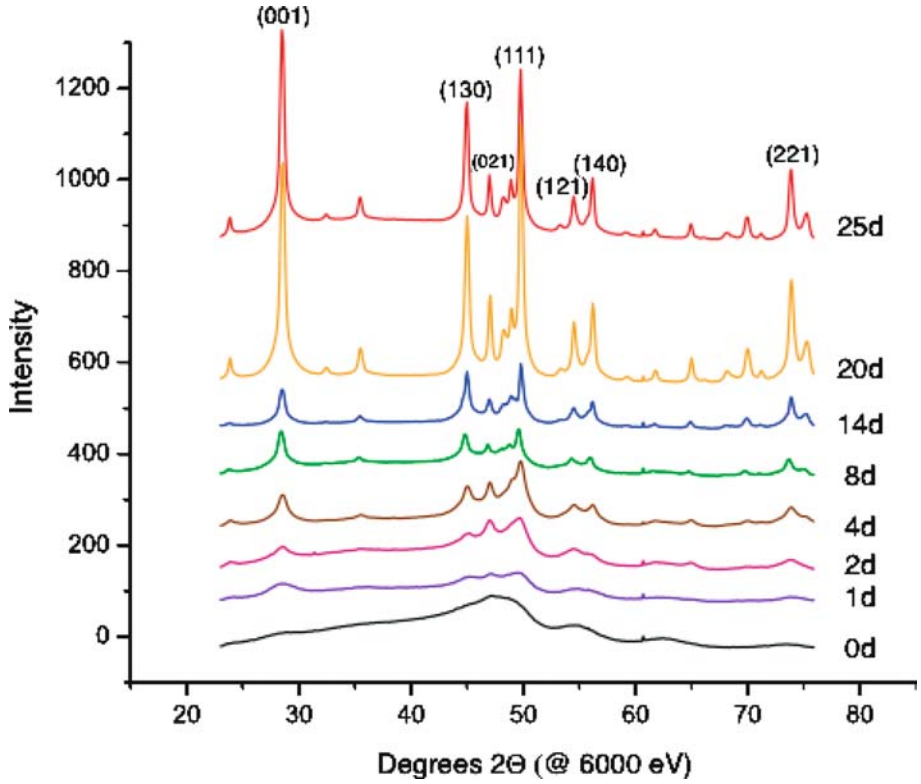

Figure 5. Synchrotron-based X-ray diffraction patterns of goethite nanoparticles after variable aging times. Over time the evolution of peaks clearly associated with goethite (as indicated by the Miller indices in the 25-day aged sample) can be observed. Data collected at beamline 7.3.3 of the Advanced Light Source.

population of nanoparticles with aging. In contrast, ripening-based growth of the nanoparticles would yield a shifting of this initial peak to greater and broader size ranges, as observed in other studies (Lo & Waite, 2000), rather than a direct decline in the population. The fact that this type of broadening and shifting appears to occur in the second population of particles suggests that ripening-based growth is perhaps a significant mechanism facilitating the continued growth of the nanoparticle aggregates.

The WAXS patterns of selected *ex situ* samples are presented in Figure 9. While considerable background subtraction issues clearly remain due to aqueous solution scattering, the evolution of progressively sharper peaks corresponding to crystalline goethite can be easily discerned. These results are comparable to the *ex situ* XRD patterns shown in the previous section, and reinforce the notion that the nanoparticles do not undergo phase transitions during the aging (or drying) process, but rather increase in size and structural ordering with time and in suspension. Ongoing work on this project involves repeating the SAXS/WAXS experiments in the presence of various metals to determine the effects of the contaminants on particle growth and size distribution.

Particle size effects on the sorption of heavy metals

The previous studies aimed to thoroughly characterize the structure, morphology, size, and growth mechanisms of nanoscale goethite in a model system setting. The subsequent series of experiments examine the effects of nanogoethite particle size on the sorption of heavy metals and metalloids. Specifically, As(V), Cu(II), Hg(II), and Zn(II) have been selected for study due to the known hazards they pose to humans as well as their prevalence in many areas of metal contamination, such as abandoned mine regions.

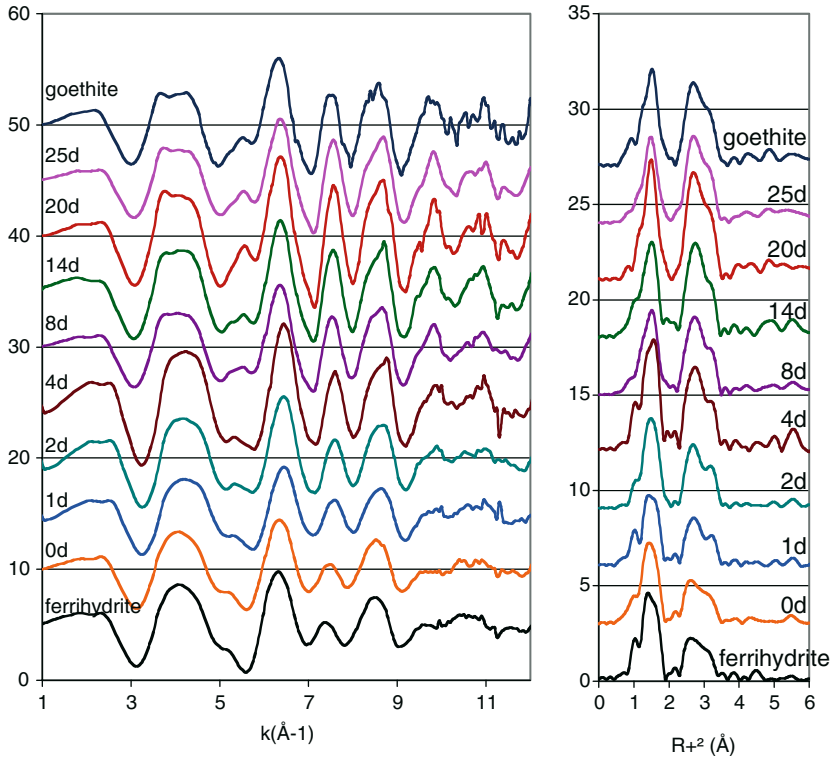

Figure 6. Fe K-edge EXAFS spectra and Fourier transforms of goethite nanoparticles after variable aging times. The continuous trends observed with aging could either be a result of a phase transition from ferrihydrite (bottom spectrum) to goethite (top spectrum) or indicate an increasing degree of structural order over time.

Nanogoethite suspensions were aged for durations expected to yield particles of 5, 25, and 75 nm average size based on earlier DLS analysis of aged samples. These differently-sized suspensions were then separately exposed to 0.5 mM initial concentrations of the aforementioned elements at pH 6 using previously-established procedures (Kim et al., 2004a, 2004b) for macroscopic uptake experiments. After 24 h reaction time, the suspensions were centrifuged and the resulting pellets prepared for analysis by As K-edge, Cu K-edge, Hg L_{III}-edge, or Zn K-edge EXAFS spectroscopy. EXAFS spectroscopy is the technique of choice for determining the speciation of sorbed and/or co-precipitated As, Cu, Zn, and Hg associated with metal oxide substrates, as has been demonstrated in numerous studies (Waychunas et al., 1993; Bochatay et al., 1997; Trivedi et al., 2001; Waychunas et al., 2002; Roberts et al., 2003; Kim et al., 2004a, 2004b). Our preliminary EXAFS studies show subtle differences in metal speciation as a function of particle size. Presented are data for Hg(II) uptake, showing that the average interatomic distances between the metal contaminant and surface iron atoms of the goethite nanoparticles appear to increase significantly at the smallest particle size (5 nm) by ~0.2 Å relative to the 25- and 75-nm particles (Figure 10). This finding suggests a substantial degree of distortion of the $Fe(O,OH)_6$ octahedra which comprise the 5-nm goethite structure, and that corresponds with the oblate morphology and increased degree of surface curvature seen in TEM images of the smallest nanoparticles compared with the more regular, rod-shaped particles formed through oriented aggregation.

To assess the effects of particle size on the extent of heavy metal sorption, sorption isotherms were generated for the uptake of Hg(II) onto 5-nm, 25-nm, and 75-nm goethite nanoparticles over a range of initial concentrations from 5 to 1000 μM and a constant solids concentration of 2.3 g/l. As

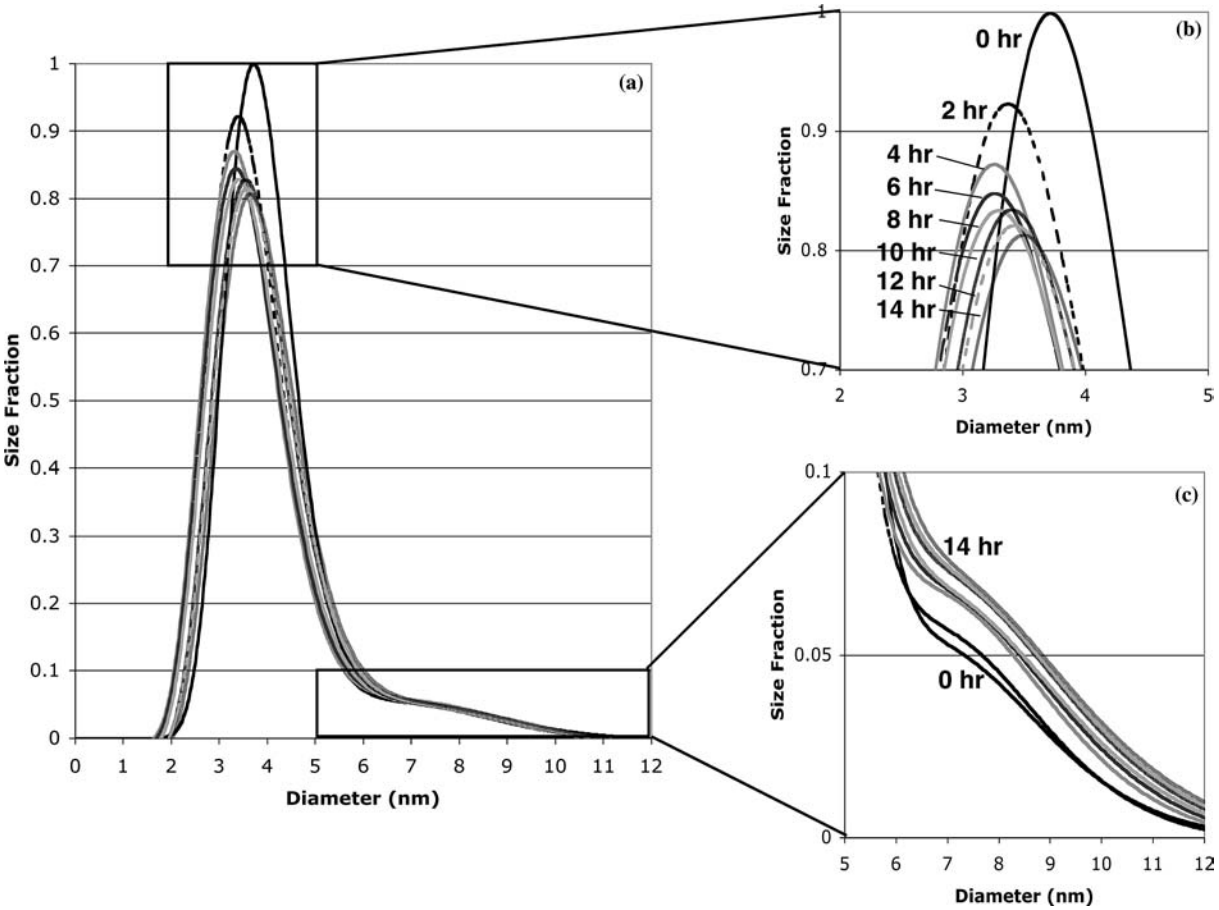

Figure 7. (a) Processed small-angle X-ray scattering (SAXS) data for the *in situ* aging of an initial 5-nm nanoparticle suspension at 70°C for 12 h, with expanded views showing (b) the decline in particles sized 2–6 nm and (c) the increase in particles >5 nm.

expected, when uptake is expressed in absolute terms (total μmol sorbed), the smallest particles, featuring the highest reactive surface area (~300 m^2/g), are shown to sorb the most Hg(II) over the entire concentration range (Figure 11a). In contrast, the largest particles, with lower surface area (130 m^2/g), have considerably less Hg(II) uptake. However, once normalized for surface area, the trend is reversed, with the smallest 5-nm particles displaying lower surface coverages at each initial Hg(II) concentration relative to the larger particles (Figure 11b). Hence in this case the smallest nanoparticle surfaces appear to have fewer and somewhat different sorption sites compared to larger particles.

These differences can be explained in the context of the earlier nanogoethite characterization work, which shows distinct changes in both morphology and structural ordering with increasing size and aging time. Referring to Figure 12, greater disordering of the $Fe(O,OH)_6$ octahedra at the surfaces of the 5-nm nanoparticles may explain both the shift in second-neighbor metal-iron distances as well as the lower surface coverages due to the reduced strength or energetic favorability of the binding sites available for metal uptake. That is, although the smallest nanoparticles can sorb the greatest amount of Hg(II) on a per mass basis, both the geometry of the sorption complexes and the degree of surface loading are altered from larger particles with more ordered surfaces. Furthermore, charge distribution has been shown to vary at the nanoscale as a function of particle aspect ratio (Rustad & Felmy, 2005), with greater

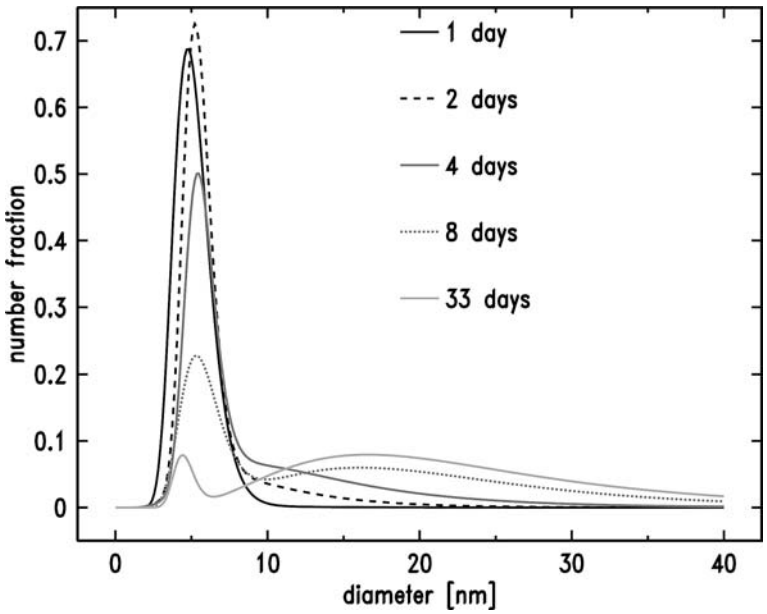

Figure 8. Processed small-angle X-ray scattering (SAXS) data for *ex situ* samples of different aging times.

charge accumulation on more acicular particles; this may also influence the formation of sorption complexes on particles over a range of size and morphology. These observations raise issues concerning the long-term stability of surface complexes formed on these smallest nanoparticles. More work is needed to quantify macroscopic uptake with different metals, and also study the desorption of metals with time as a function of particle size. These studies clearly demonstrate that nanoparticles display altered metal sorption properties relative to larger counterparts.

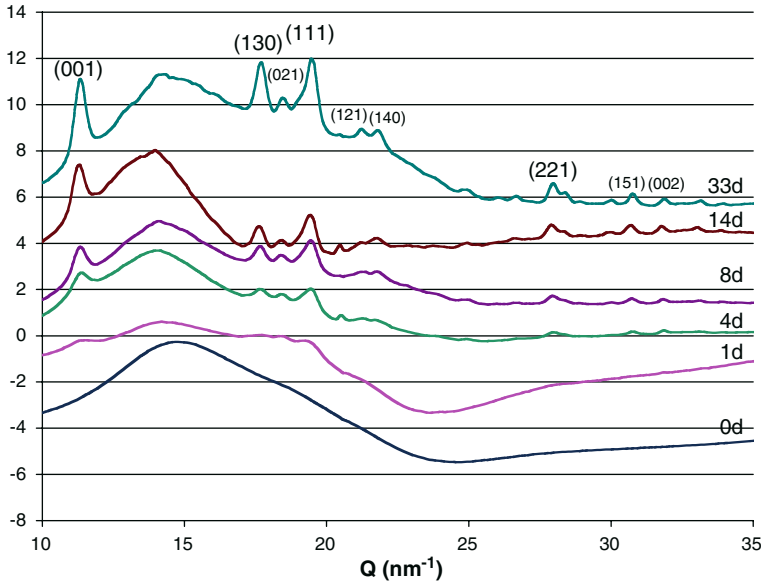

Figure 9. Wide-angle X-ray scattering (WAXS) data for samples of different aging times.

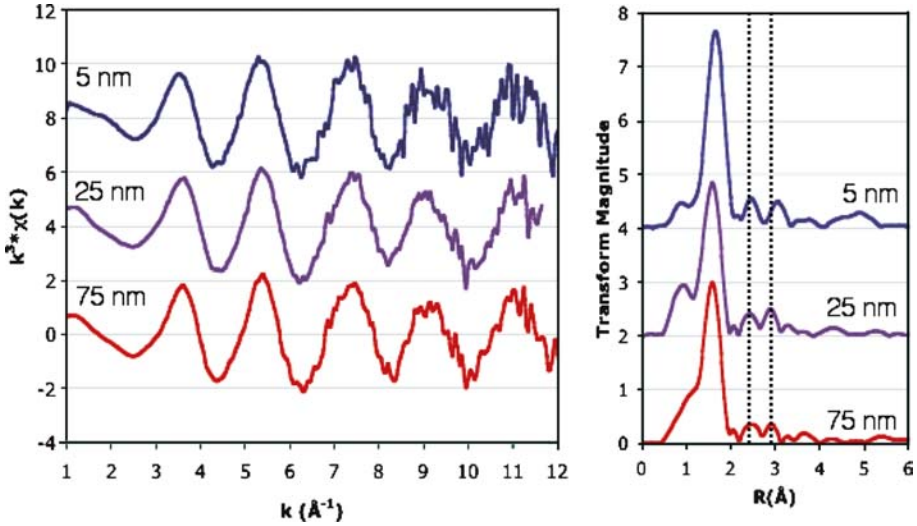

Figure 10. Hg L_{III}-edge EXAFS and corresponding Fourier transforms of Hg(II) sorbed to goethite nanoparticles of 5, 25, and 75 nm average diameter. Guidelines on the Fourier transforms reveal differences in the most distant (Hg–Fe) interatomic distances when Hg(II) is sorbed to the smallest 5-nm particles.

Retention of heavy metals during aggregation-based nanoparticle growth

As discussed earlier, the effects of aggregation-based nanoparticle growth in the presence of and/or following the sorption of metals to their surfaces may have significant implications for both the fate of the contaminants as well as the growth kinetics of the nanoparticles themselves. To begin to assess these effects, macroscopic uptake experiments were conducted under similar conditions to those in the work just described. However, instead of introducing the metals to the nanoparticles after they had been aged to the desired size, they were introduced into the initial nanoparticle suspension which was subsequently allowed to age at 90°C

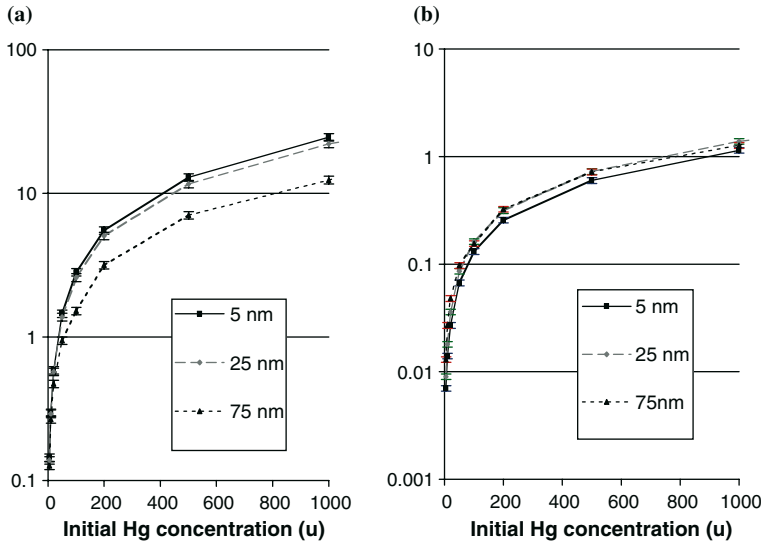

Figure 11. Macroscopic uptake data of Hg(II) onto goethite nanoparticles of different sizes, showing (a) uptake expressed in terms of total μmol sorbed and (b) uptake normalized for surface area and expressed as μmol/m^2.

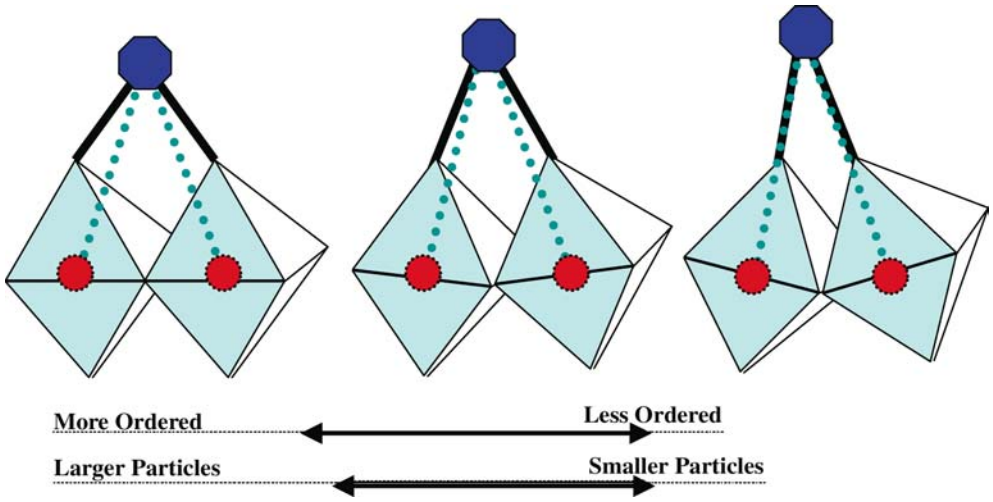

Figure 12. Schematic diagram showing distortion of $Fe(O,OH)_6$ octahedra, the building blocks of the goethite structure, thought to occur as particle size decreases and surface curvature/disorder increases.

with periodic sample aliquots collected over the course of 24 h. EXAFS spectroscopy of the resulting solids was then conducted in order to determine if the mode of uptake had changed over this short time span.

Figure 13 shows the results of one of these sets of metal/aging experiments, conducted in the presence of Zn(II). A clear trend in both the EXAFS and Fourier transforms can be observed with time; in particular, the substantial increase in the amplitude of the second-neighbor features in the Fourier transform (representing Zn–Fe and/or Zn–Zn interactions) indicates greater structural ordering of the Zn and/or a larger

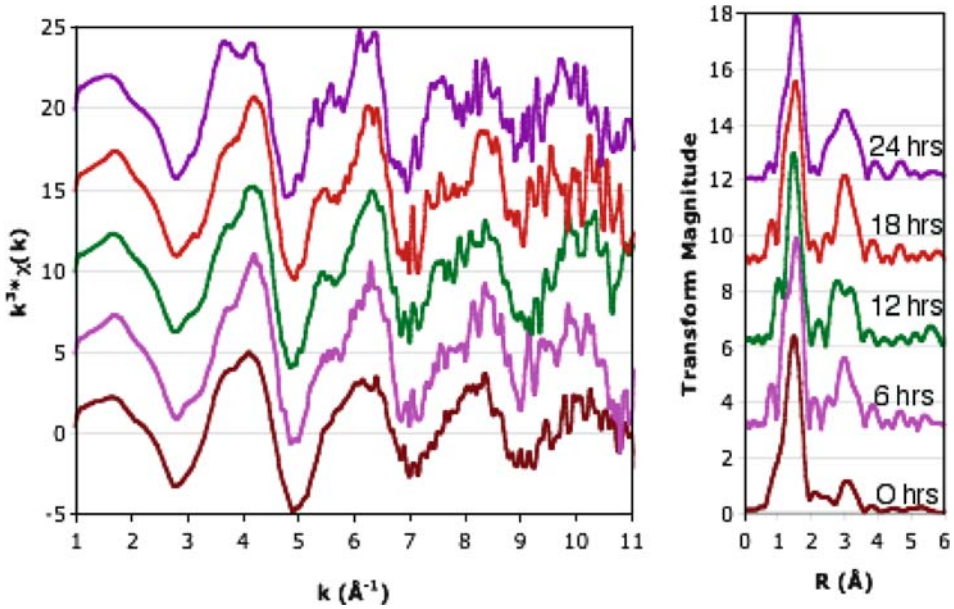

Figure 13. Zn K-edge EXAFS and Fourier transforms of 5-nm goethite nanoparticles aged in the presence of Zn(II) over the course of 24 h. The significant increase in the amplitude of the second-neighbor peaks in the Fourier transforms indicates an increase in structural order consistent with structural incorporation and/or (co)precipitation of Zn.

average number of neighboring iron or zinc atoms. This suggests that Zn has either become more structurally incorporated within the substrate or has formed a secondary precipitate phase as a direct result of the nanoparticle growth conditions. It is worth noting that the spectra of Zn(II) sorbed to goethite nanoparticles that have been allowed to aggregate for the same period of time, but in the absence of metals, does not at all resemble that of the aged sample shown in Figure 13. Hence the dramatic changes observed are almost exclusively a byproduct of the aggregation-based growth process of nanoparticles in the presence of metals. This process is considerably more relevant to natural systems, where iron oxyhydroxide formation and growth occurs not in isolation but in the presence of a host of organic and inorganic species, including metals, that may influence particle growth rates and mechanisms as well as the fate of the metal contaminants during the growth process.

Whether the changes observed in the EXAFS data correspond to the structural incorporation of Zn within the goethite structure or some form of Zn (co)precipitation, each represents a different mode of uptake from the inner-sphere surface adsorption observed in macroscopic studies (Trivedi et al., 2001; Waychunas et al., 2002). While the differences in the permanence and reversibility of metal sorption as a result of these different sequestration mechanisms are not yet known, expectations of improved metal pollutant containment through such processes may underscore the potential of nanoparticle aggregation as a viable strategy for the removal of metals from solution and storage in the solid phase.

From our other metal/aging experiments, similar differences are observed among EXAFS spectra of Hg(II) sorbed to the goethite nanoparticles before and after 24 h of aging, while As(V) and Cu(II) exhibit only subtle changes (not shown). This element-specific behavior is consistent with a host of mostly macroscopic studies (Spadini et al., 1994; Ford et al., 1997, 1999; Martinez & McBride, 1998, 2001; Karthikeyan et al., 1999a, 1999b; Trivedi et al., 2001; Ford, 2002; Waychunas et al., 2002) which indicate evidence for structural incorporation of certain metal cations (e.g., Cu(II) Mn(II), Ni(II), Zn(II)) and minimal incorporation of others (e.g., Cd(II), Pb(II)) either during initial iron oxyhydroxide formation or when exposed to iron oxyhydroxides that are allowed to undergo phase transitions from ferrihydrite (HFO) to goethite or hematite (α-Fe_2O_3). Ion size, preferred coordination chemistry, and steric effects may distinguish between metals that are more likely to form (co)precipitates and those that are not.

Nanoparticle studies of other FeOX materials

Nanoparticle hematite has been studied for many years because of its interesting magnetic properties (e.g., Bodker & Morup, 2000; Gee et al., 2004). Hematite is a weak ferromagnet between the Morin and Neel transition temperatures ($\sim$260 and $\sim$956 K, respectively, in bulk), and is subject to superparamagnetic relaxation effects as particle size decreases. The mode of preparation, cell dimensions and stoichiometry all affect magnetic properties (Dang et al., 1998). The Morin transition temperature is found to decrease by more than 40 K with decreasing particle size, and there are also continuous changes in magnetic anisotropy. Study of nanoparticle hematite structure by X-ray absorption near-edge structure (XANES) spectroscopy suggests that surface sites are distorted with respect to bulk sites, and may even have lower oxygen coordination (Chen et al., 2002), though this is not observed on large single crystal surfaces (Trainor et al., 2004). Quantum confinement has been demonstrated in hematite nanorods (Guo et al., 2004) using resonant inelastic X-ray scattering (RIXS). Specifically, the band gap in 50 nm rods was found to increase from the 2.1 eV in bulk hematite, to 2.5 eV. Perhaps of more importance to environmental chemistry, are studies of aqueous photochemical effects. Lindgren et al. (2002) found that hematite nanorods were more efficient at water oxidation than bulk hematite, though the material may have practical limits due to slow reaction kinetics at the water interface. Madden and Hochella (2005) observed related phenomena in nanoparticulate hematite, with a doubling of oxidation rate for 9 nm particles compared to bulk. As photochemical water oxidation results in Fe valence reduction at the particle surface, there will be increased aqueous ferrous ion and probable changes in sorption processes. Such work suggests that similar processes may be important in other nanosize FeOX materials.

Akaganeite (β-FeOOH) nanofibers with extreme aspect ratios of 1088:1 (length/width) are observed to form in the vicinity of bacteria under certain conditions, and are believed to be favored due to templating effects by polysaccharide molecules (Chan et al., 2004). This observation highlights the possible importance of biological interactions with FeOX precipitates to produce unusual structures, topologies and phases, particularly at the nano size regime. Akaganeite is not a pure FeOX material, and requires a small amount of bound Cl^- or other ion in its tunnel structure to gain electrostatic stabilization. Nanocrystals can be synthesized by a variety of recipes/methods, and nanocrystals of size 2–6 nm have been prepared (Deliyanni et al., 2001), however little detailed structural characterization has been done on such materials.

Magnetite is a highly magnetic mixed valence spinel-structure FeOX phase that has been studied for its magnetic properties, high electrical conductivity, cellular production, and many technological applications. Although unstable in most aerobic surface environments with respect to maghemite, hematite or goethite, it can be formed inorganically in deeper sediments where reducing conditions obtain (e.g., via alteration of olivine in oceanic basalts). Nanoparticulate magnetite is formed in abundance in many aqueous environments as the result of microbial activity. Chains of intracellular magnetically single domain magnetite are synthesized within the magnetosomes of many bacteria. In addition, dissimilatory processes during anaerobic respiration lead to formation of large volumes of very finely particulate extracellular magnetite (Bazylinksi & Moskowitz, 1997). Such nanocrystals can be ''farmed'' for use in medical and biotechnology applications (Matsunaga & Okamura, 2002) such as for chemiluminescent enzyme immunoassay using antibody–magnetite coupled nanoparticles. As a mixed-valence oxide, the redox properties of magnetite particles have been examined in several studies. Aqueous chromate anions, which contain toxic Cr(VI), can be reduced by magnetite surfaces to the less toxic Cr(III) valence state (Peterson et al., 1997), and this has led to consideration of magnetite as a remediation tool for chromate in water systems. Aggregated magnetite nanoparticles have also been suggested as effective decontamination agents for radioactive wastes containing Cs (Ambashta et al., 2003). In such scenarios, the magnetite nanoparticles are chemically processed to connect sorbate-selective agents to their surfaces. Once sorption occurs, the magnetite particles can be removed by high field gradient methods. This is a promising technology for water purification and other contaminant remediation (Moeser et al., 2004). Magnetite nanoparticles are also utilized in ferrofluidic liquids that have applications in many types of bearings and engineering applications. Despite this attention there remains less definitive characterization of nanomagnetite surface and bulk structure, chemistry (including the valence ratios of Fe at the surface), surface relaxations, or sorption properties.

Ferrihydrite may not be a single phase, but rather a continuous series or set of phases, with varying degrees of structural order. It does not occur in crystallites larger than submicron size, and structural characterization has been debated in the literature for some time (Carlson & Schwertmann, 1981; Drits et al., 1993; Janney et al., 2000). The most disordered variety, referred to as ''2-line'' ferrihydrite, hydrous ferric oxide, or HFO, usually has grain sizes of only a few nm. The most ordered variety is termed ''6-line'' ferrihydrite (these designations referring to the number of major XRD peaks observed in the powder pattern), and intermediate structures may consist of mixtures or still other structural variants. With nanoparticulate grain size and thus large effective surface areas, HFO can be a major factor in contaminant (and nutrient) sorption and transport, despite the instability of the phase with respect to conversion to goethite or hematite (Hochella et al., 1999). Much work has been done on the sorption properties of HFO as a bulk nanoparticulate phase (Dzombak & Morel, 1990), but the effects of grain size variation on properties are not well known. An interesting aspect of HFO sorption is the effect of significant sorption of strongly bound complexes such as silica and arsenate (Fuller et al., 1993; Waychunas et al., 1993; Rea et al., 1994; Ford, 2002). In these cases the growth of the HFO particles is poisoned, and the transformation kinetics are slowed.

Schwertmannite is a poorly crystallized iron oxyhydroxide with essential sulfate that forms in acid mine drainage environments at low pH values (Bigham et al., 1996). Its structure is

supposedly related to that of akaganeite, but most recent work suggests that it may more closely resemble a more disordered form of ferrihydrite (Loan et al., 2004). Always formed as sub-micron crystallites, it is an important agent for sorption of metal contaminants, as well as a carrier of significant sulfate, in acid mine drainage situations.

Conclusions

Owing to their large surface area, tendency to aggregate as part of their growth process, and possible altered chemical and physical properties relative to bulk crystallites, nanoparticulate FeOX minerals may be extremely influential in natural geochemical processes. We have detailed many of the ways in which nanoparticles may differ from their bulk counterparts, and demonstrated that some of these effects are observed in sorption processes with nanogoethite particles both in adsorption and coprecipitation experiments. Much more work needs to be done to understand nanogoethite reactivity, including combined sorption and redox experiments, studies of aggregation geometry and both surface complex and fluid entrapment, and competitive studies of sorption and dissolution. Similarly, other important natural FeOX nanophases such as hematite, ferrihydrite and magnetite also require additional detailed investigation. In addition, the FeOX phases represent only one set of naturally occurring nanoparticles that can have major environmental influence. Others include the manganese oxides and hydroxides, aluminum hydroxides, and both silica-based and anionic clay minerals. Studies of the type described herein are increasing in number, but there remains a large void in the characterization and comprehension of nanomineral reactivity in natural systems. Ultimately, geochemical models will need to include the transport of nanoparticulates in complex natural pore systems within sediments and strata. This is another area of investigation that is just beginning, but which is the next crucial step in utilizing the knowledge gained on nanoparticulate behavior to address actual real world problems. Such a level of natural system modeling will require improved understanding of both nanoparticle properties and microporous flow character.

Acknowledgements

We thank Gary Sposito for use of his DLS system and Andy Yang for assistance during its use. Nobumichi Tamura and Bryan Valek at the ALS provided helpful support during the synchrotron-based XRD data collection at BL 7.3.3. We would also like to acknowledge the assistance of APS staff, particularly Steve Weigand at DND-CAT for help with the SAXS/WAXS studies and Matt Newville at GSECARS for support during the EXAFS experiments. Mike Toney (SSRL) provided data reduction of the raw SAXS data. Banfield and Waychunas received support from the U.S. Department of Energy, Office of Basic Energy Sciences. Kim was supported by the Lawrence Berkeley National Laboratory's Laboratory Directed Research and Development (LDRD) program. Use of the Advanced Photon Source was supported by the U. S. Department of Energy, Office of Science, Office of Basic Energy Sciences, under Contract No. W-31-109-Eng-38. The Advanced Light Source is supported by the Director, Office of Science, Office of Basic Energy Sciences, Materials Sciences Division, of the U.S. Department of Energy under Contract No. DE-AC03-76SF00098 at Lawrence Berkeley National Laboratory.

References

Ambashta R.D., P.K. Wattal, S. Singh & D. Bahadur, 2003. Nano-aggregates of hexacyanoferrate-loaded magnetite for removal of cesium from radioactive wastes. J. Mag. Magn. Mat. 267, 335–340.

Baes C.F. & R.E. Mesmer, 1976. The Hydrolysis of Cations. Malabar, FL Krieger Publishing.

Banfield J.F. & H. Zhang, 2001. Nanoparticles in the Environment. Rev. Mineral. Geochem. 44, 1–58.

Banfield J.F., S.A. Welch, H.Z. Zhang, T.T. Ebert & R.L. Penn, 2000. Aggregation-based crystal growth and microstructure development in natural iron oxyhydroxide biomineralization products. Science 289(5480), 751–754.

Bargar J.R., G.E. Brown Jr. & G.A. Parks, 1997. Surface complexation of Pb(II) at oxide–water interfaces: II. XAFS and bond-valence determination of mononuclear Pb(II) sorption products and surface functional groups on iron oxides. Geochim. Cosmochim. Acta 61(13), 2639–2652.

Barker W.W., S.A. Welch, S. Chu & J.F. Banfield, 1998. Experimental observations of the effects of bacteria on aluminosilicate weathering. Am. Mineral. 83, 1551–1563.

Bochatay L., P. Persson, L. Lovgren & G.E. Brown, 1997. XAFS study of Cu(II) at the water–goethite (alpha-FeOOH) interface. Journal De Physique IV 7(C2/pt.2), 819–820.

Bodker F. & S. Morup, 2000. Size dependence of the properties of hematite nanoparticles. Europhys. Lett. 52, 217–223.

Boily J.F., J. Lutzenkirchen, O. Balmes, J. Beattie & S. Sjoberg, 2001. Modeling proton binding at the goethite (α-FeOOH)-water interface. Colloid. Surfaces A 179, 11–27.

Brown I.D. & R.D. Shannon, 1973. Empirical bond-strength–bond-length curves for oxides. Acta Cryst. A 29, 266–282.

Brown G.E. & N.C. Sturchio, 2002. An overview of synchrotron radiation applications to low temperature geochemistry and environmental science. Rev. Mineral. Geochem. 49, 1–115.

Brus L.E., 1983. A simple model for the ionization potential, electron affinity, and aqueous redox potentials of small semiconductor crystallites. J. Chem. Phys. 79, 5566–5571.

Carlson L. & U. Schwertmann, 1981. Natural ferrihydrites in surface deposits from Finland and their association with silica. Geochim. Cosmochim. Acta 45, 421–429.

Chan C.S., G. De Stasio, S.A. Welch, M. Girasole, B.H. Frazer, M.V. Nesterova, S. Fakra & J.F. Banfield, 2004. Microbial polysaccharides template assembly of nanocrystal fibers. Science 303(5664), 1656–1658.

Chen L.X., T. Liu, M.C. Thurnauer, R. Csencsits & T. Rajh, 2002. Fe_2O_3 nanoparticle structures investigated by X-ray absorption near-edge structure, surface modifications, and model calculations. J. Phys. Chem. B 106, 8539–8546.

Cheng B., J. Kong, J. Luo & Y. Dong, 1993. Mater. Sci. Prog. 7, 240–243 (in Chinese).

Combes J.-M., A. Manceau, G. Calas & J.Y. Bottero, 1989. Formation of ferric oxides from aqueous solutions: A polyhedral approach by X-ray absorption spectroscopy. I. Hydrolysis and formation of ferric gels oxide crystallization and the influence on coprecipitated arsenate. Environ. Sci. Tech. 36, 2459–2463.

Dang M.Z., D.G. Rancourt, J.E. Dutrizac, G. Lamarche & R. Provencher, 1998. Interplay of surface conditions, particle size, stoichiometry, cell parameters, and magnetism in synthetic hematite-like minerals. Hyperfine Interact. 117, 271–319.

Davis J.A. & D.B. Kent, 1990. Surface complexation modeling in aqueous geochemistry. Rev. Mineral. 23, 177–260.

Deliyanni E.A., D.N. Baboyannakis, A.I. Zouboulis, K.A. Matis & L. Nalbandian, 2001. Akaganeite-type β-FeO(OH) nanocrystals: Preparation and characterization. Microporous Mesoporous Mater. 42, 49–57.

Drits V.A., B.A. Sakharov, A.L. Salyn & A. Manceau, 1993. Structural model of ferrihydrite. Clay Minerals 28, 185–207.

Dzombak D.A. & F.M.M. Morel, 1990. Surface Complexation Modeling: Hydrous Ferric Oxide. New York John Wiley.

Edwards K.J., P.L. Bond, G.K. Druschel, M.M. McGuire, R.J. Hamers & J.F. Banfield, 2000. Geochemical and biological aspects of sulfide mineral dissolution: lessons from Iron Mountain, California. Chem. Geol. 169, 383–397.

Eng P.J., T.P. Trainor, G.E. Brown, G.A. Waychunas, M. Newville, S.R. Sutton & M.L. Rivers, 2000. Structure of the hydrated α-Al_2O_3 surface. Science 288, 1029–1033.

Ford R.G., 2002. Rates of hydrous ferric oxide crystallization and the influence on coprecipitated arsenate. Environ. Sci. Tech. 36(11), 2459–2463.

Ford R.G., P.M. Bertsch & K.J. Farley, 1997. Changes in transition and heavy metal partitioning during hydrous iron oxide aging. Environ. Sci. Tech. 31(7), 2028–2033.

Ford R.G., K.M. Kemner & P.M. Bertsch, 1999. Influence of sorbate-sorbent interactions on the crystallization kinetics of nickel– and lead–ferrihydrite coprecipitates. Geochim. Cosmochim. Act. 63(1), 39–48.

Fuller C.C., J.A. Davis & G.A. Waychunas, 1993. Surface chemistry of ferrihydrite: Part 2. Kinetics of arsenate adsorption and coprecipitation. Geochim. Cosmochim. Acta 57, 2271–2282.

Gee S., Y. Hong, J. Sur, D. Erickson, M. Park & F. Jeffers, 2004. Spin orientation of hematite nanoparticles during the Morin transition. IEEE Trans. Magn. 40, 2691–2693.

Gilbert B., F. Huang, H Zhang, G. Waychunas & J.F. Banfield, 2004. Nanoparticles: Strained and stiff. Science 305, 651–654.

Gilbert B., H.Z. Zhang, F. Huang, M.P. Finnegan, G.A. Waychunas & J.F. Banfield, 2003. Special phase transformation and crystal growth pathways observed in nanoparticles. Geochem. Trans. 4, 20–27.

Grätzel M., 1989. In: Serpone N. & Pelizzetti E. eds. Photocatalysis-Fundamentals and Applications. Wiley-Interscience, New York, pp. 123–157.

Guo J.-H., L. Vayssieres, C. Sathe, S. Butorin & J. Nordgren, 2004. Quantum confinement observed in a α-Fe_2O_3 nanorod-array. www-als.lbl.gov/als/compendium/ AbstractManager/uploads/01082.pdf.

Guyodo Y., A. Mostrom, R.L. Penn & S.K. Banerjee, 2003. From nanodots to nanorods: Oriented aggregation and magnetic evolution of nanocrystalline goethite. Geophys. Res. Lett. 30(10), 1512 .

Hayes K.F. & J.O. Leckie, 1987. Modeling ionic strength effects on cation sorption at hydrous oxide/solution interfaces. J. Colloid Interface Sci. 115, 564–572.

Hochella M.F., J.N. Moore, U. Golla & A. Putnis, 1999. A TEM study of samples from acid mine drainage systems: Metal–mineral association with implications for transport. Geochim. Cosmochim. Acta 63, 3395–3406.

Hoffman, A.J. & M.R. Hoffman, 1993. In: Ollis D.F. & Al-Ekabi H. eds. Purification and Treatment of Water and Air. Elsevier Science Publishers, Amsterdam, pp. 155–162.

Huang F., H.Z. Zhang & J.F. Banfield, 2003. Two-stage crystal-growth kinetics observed during hydrothermal coarsening of nanocrystalline ZnS. Nano Lett. 3(3), 373–378.

Janney D.E., J.M. Cowley & P.R. Buseck, 2000. Structure of synthetic 2-line ferrihydrite by electron nanodiffraction. Am. Mineral. 85, 1180–1187.

Karthikeyan K.G. & H.A. Elliott, 1999a. Surface complexation modeling of copper sorption by hydrous oxides of iron and aluminum. J. Colloid Interface Sci. 220(1), 88–95.

Karthikeyan K.G., H.A. Elliott & J. Chorover, 1999b. Role of surface precipitation in copper sorption by the hydrous oxides of iron and aluminum. J. Colloid Interface Sci. 209(1), 72–78.

Kim C.S., J.J. Rytuba & G.E. Brown Jr., 2004a. EXAFS study of mercury(II) sorption to Fe- and Al-(hydr)oxides: I. Effects of pH. J. Colloid Interface Sci. 271, 1–15.

Kim C.S., J.J. Rytuba & G.E. Brown Jr., 2004b. EXAFS study of mercury(II) sorption to Fe- and Al-(hydr)oxides: II. Effects of chloride and sulfate. J. Colloid Interface Sci. 270, 9–20.

Korgel B.A. & H.G. Monbouquette, 1997. Quantum confinement effects enable photocatalyzed nitrate reduction at neutral pH using CdS nanocrystals. J. Phys. Chem. B 101, 5010–5017.

Lindgren T., H. Wang, N. Beermann, L. Vayssieres, A. Hagfeldt & S.-E. Linquist, 2002. Aqueous photoelectrochemistry of hematite nanorod array. Sol. Energy Mater. Sol. Cells 71, 231–243.

Lo B. & T.D. Waite, 2000. Structure of hydrous ferric oxide aggregates. J. Colloid Interface Sci. 222, 83–89.

Loan M., J.M. Cowley, R. Hart & G.M. Parkinson, 2004. Evidence on the structure of synthetic schwertmannite. Am. Mineral. 89, 1735–1742.

Madden A.S. & M.F. Hochella, 2005. A test of geochemical reactivity as a function of mineral size: Manganese oxidation promoted by hematite nanoparticles. Geochem. Cosmochim. Acta 69, 389–398.

Manceau A. & L. Charlet, 1994. The mechanism of selenate adsorption on goethite and hydrous ferric oxide. J. Colloid Interface Sci. 168, 87–93.

Manceau A., K.L. Nagy, L. Spadini & K.V. Ragnarsdottir, 2000. Influence of anionic layer structure of Fe-oxyhydroxides on the structure of Cd surface complexes. J. Colloid Interface Sci. 228, 306–316.

Manceau A., L. Charlet, M.C. Boisset, B. Didier & L. Spadini, 1992. Sorption and speciation of heavy metals on hydrous Fe and Mn oxides. Appl. Clay Sci. 7, 201–223.

Martinez C.E. & M.B. McBride, 1998. Solubility of Cd^{2+}, Cu^{2+}, Pb^{2+}, and Zn^{2+} in aged coprecipitates with amorphous iron hydroxides. Environ. Sci. Tech. 32(6), 743–748.

Martinez C.E. & M.B. McBride, 2001. Cd, Cu, Pb, and Zn coprecipitates in Fe oxide formed at different pH: Aging effects on metal solubility and extractability by citrate. Environ. Toxicol. Chem. 20(1), 122–126.

Matsunaga T. & Y. Okamura, 2002. Molecular mechanism of bacterial magnetite formation and its application. Biological and Biomimetic materials. Mater. Res. Soc. Symposium Proc. 724, 11–24.

Moeser G.D., K.A. Roach, W.H. Green, T.A. Hatton & P.E. Laibinis, 2004. High-gradient magnetic separation of coated magnetic nanoparticles. AICHE J. 50, 2835–2848.

Myneni S., G.A. Waychunas, G.E. Brown & S.J. Traina, 2004. Understanding the speciation of oxoanions in aquatic systems (to be submitted).

Navrotsky A., 2001. Thermochemistry of nanomaterials. Rev. Mineral. Geochem. 44, 73–103.

Osbourn G.C., 1983. $In_xGa_{1-x}As$-$In_yGa_{1-y}As$ strained-layer superlattices: A proposal for new, useful electronic materials. Phys. Rev. B 27, 5126–5128.

Penn R.L., 2004. Kinetics of oriented aggregation. J. Phys. Chem. B 108(34), 12707–12712.

Penn R.L. & J.F. Banfield, 1998. Oriented attachment and growth, twinning, polytypism, and formation of metastable phases: Insights from nanocrystalline TiO_2. Am. Mineral. 83(9–10), 1077–1082.

Penn R.L., G. Oskam, T.J. Strathmann, P.C. Searson, A.T. Stone & D.R. Veblen, 2001. Epitaxial assembly in aged colloids. J. Phys. Chem. B 105(11), 2177–2182.

Peterson M.L., G.E. Brown, G.A. Parks & C.L. Stein, 1997. Differential redox and sorption of Cr(III/VI) on natural silicate and oxide minerals: EXAFS and XANES results. Geochim. Cosmochim. Acta 61(16), 3399–3412.

Qu F., R.H. Oliveira & P.C. Morais, 2004. Effects of nanocrystal shape on the surface charge density of ionic colloidal nanoparticles. J. Magn. Magn. Mater. 272–276, 1668–1669.

Rea B.A., J.A. Davis & G.A. Waychunas, 1994. Studies of the reactivity of the ferrihydrite surface by iron isotope exchange and Mössbauer spectroscopy. Clays Clay Mineral. 42, 23–34.

Roberts D.R., R.G. Ford & D.L. Sparks, 2003. Kinetics and mechanisms of Zn complexation on metal oxides using EXAFS spectroscopy. J. Colloid Interface Sci. 263(2), 364–376.

Rustad J.R. & A.R. Felmy, 2005. The influence of edge sites on the development of surface charge on goethite nanoparticles: A molecular dynamics investigation. Geochim. Cosmochim. Acta 69(6), 1405–1411.

Savage K.S., T.N. Tingle, P.A. O'Day, G.A. Waychunas & D.K. Bird, 2000. Arsenic speciation in pyrite and secondary weathering phases, Mother Lode Gold District, Tuolumne County, California. Appl. Geochem. 15, 1219–1244.

Spadini L., A. Manceau, P.W. Schindler & L. Charlet, 1994. Structure and stability of Cd^{2+} surface complexes on ferric oxides. 1. Results from EXAFS spectroscopy. J. Colloid Interface Sci. 168(1), 73–86.

Sposito G., 1986. On distinguishing adsorption from surface precipitation. In: Davis J.A. & Hayes K.F. eds. Geochemical Processes at Mineral Surfaces. ACS Symposium Ser 323, Amer Chem Soc, Washington, D.C. pp. 217–228.

Straub K.L., M. Benz, B. Schink & F. Widdel, 1996. Anaerobic, nitrate-dependent microbial oxidation of ferrous iron. Appl. Environ. Microbiol. 62, 1458–1460.

Toyoda T. & I. Tsuboya, 2003. Apparent band gap energies of mixed TiO_2 nanocrystals with rutile and anatase structures characterized with photoacustic spectroscopy. Rev. Sci. Instrum. 74, 781–783.

Trainor T.P., A.M. Chaka, P.J. Eng, M. Newville, G.A. Waychunas, J.G. Catalano & Brown G.E. (2004) et al. Structure and reactivity of the hydrated Surface. Surf. Sci. 573, 204–224.

Trivedi P., L. Axe & T.A. Tyson, 2001. An analysis of zinc sorption to amorphous versus crystalline iron oxides using XAS. J. Colloid Interface Sci. 244(2), 230–238.

Tsai M.H., S.Y. Chen & P. Shen, 2004. Imperfect oriented attachment: Accretion and defect generation of nanosize rutile condensates. Nano Lett. 4(7), 1197–1201.

Tsunekawa S., S. Ito, T. More, K. Ishikawa, Z.-Q. Li & Y. Kawazoe, 2000a. Critical size and anomalous lattice

expansion in nanocrystalline $BaTiO_3$ particles. Phys. Rev. B 62, 3065–3070.

Tsunekawa S., K. Ishikawa Li, Y. Kawazoe & A. Kasuya, 2000b. Origin of anomalous lattice expansion in oxide nanoparticles. Phys. Rev. Lett. 85, 3440–3443.

van der Zee C., D.R. Roberts, D.G. Rancourt & C.P. Slomp, 2003. Nanogoethite is the dominant reactive oxyhydroxide phase in lake and marine sediments. Geology 31(11), 993–996.

Warren B.E., 1968. X-Ray Diffraction. Addison-Wesley Reading, Mass. p. 381.

Waychunas G.A., C.C. Fuller & J.A. Davis, 2002. Surface complexation and precipitate geometry for aqueous Zn(II) sorption on ferrihydrite I: X-ray absorption extended fine structure spectroscopy analysis. Geochim. Cosmochim. Acta 66(7), 1119–1137.

Waychunas G.A., B.A. Rea, C.C. Fuller & J.A. Davis, 1993. Surface chemistry of ferrihydrite: 1. EXAFS studies of the geometry of coprecipitated and adsorbed arsenate. Geochim. Cosmochim. Acta 57(10), 2251–2269.

White A.F. & S.L. Brantley, 1995. Chemical Weathering rates of silicate minerals. Rev. Mineral. 31, 1–583.

Wiesendanger R., I.V. Shvets & J.M.D. Coey, 1994. Wigner glass on the magnetite (001) surface observed by scanning-tunneling microscopy with a ferromagnetic tip. J. Vac. Sci. Tech. B 12, 2118–2121.

Zhang H., R.L. Penn, R.J. Hamers & J.F. Banfield, 1999. Enhanced adsorption of molecules on surfaces of nanocrystalline particles. J. Phys. Chem. B 103, 4656–4662.

Zhang H., F. Huang, B. Gilbert & J.F. Banfield, 2003. Molecular dynamics simulations, thermodynamic analysis and experimental study of phase stability of zinc sulfide nanoparticles. J. Phys. Chem. B 107, 13051–13060.

Zhao J., F.E. Huggins, Z. Feng & G.P. Huffman, 1994. Ferrihydrite: Surface structure and its effects on phase transformations. Clays Clay Mineral. 42, 737–746.

Zhang H.Z. & J.F. Banfield, 2004. Aggregation, coarsening, and phase transformation in ZnS nanoparticles studied by molecular dynamics simulations. Nano Lett. 4(4), 713–718.